Available online at www.sciencedirect.com
SCIENCE DIRECT
Journal of Colloid and Interface Science 298 (2006) 132–144
JOURNAL OF Colloid and Interface Science
www.elsevier.com/locate/jcis

Adsorption-induced fibronectin aggregation and fibrillogenesis

Delphine Pellenc [a,1,*], Hugues Berry [a,b], Olivier Gallet [a]

[a] *ERRMECe, Université de Cergy-Pontoise, 2 avenue Adolphe Chauvin BP 222, 95302 Pontoise cedex, France*
[b] *Team Alchemy, INRIA Futurs, 4 rue Jacques Monod, 91893 Orsay cedex, France*

Received 2 August 2005; accepted 25 November 2005

Available online 20 December 2005

Abstract

Fibronectin (Fn), a high molecular weight glycoprotein, is a central element of extracellular matrix architecture that is involved in several fundamental cell processes. In the context of bone biology, little is known about the influence of the mineral surface on fibronectin supramolecular assembly. We investigate fibronectin morphological properties induced by its adsorption onto a model mineral matrix of hydroxyapatite (HA). Fibronectin adsorption onto HA spontaneously induces its aggregation and fibrillation. In some cases, fibronectin fibrils are even found connected into a dense network that is close to the matrix synthesized by cultured cells. Fibronectin adsorption-induced self-assembly is a time-dependant process that is sensitive to bulk concentration. The N-terminal domain of the protein, known to be implicated in its self-association, does not significantly inhibit the protein self-assembly while increasing ionic strength in the bulk alters both aggregation and fibrillation. The addition of a non-ionic surfactant during adsorption tends to promote aggregation with respect to fibrillation. Ultimately, fibronectin fibrils appear to be partially structured like amyloid fibrils as shown by thioflavine T staining. Taken together, our results suggest that there might be more than one single organization route involved in fibronectin self-assembly onto hydroxyapatite. The underlying mechanisms are discussed with respect to Fn conformation, Fn/surface and Fn/Fn interactions, and a model of fibronectin fibrillogenesis onto hydroxyapatite is proposed.

Keywords: Fibronectin; Aggregation; Fibrillogenesis; Protein adsorption; Hydroxyapatite; Biomaterials

1. Introduction

Fibronectin (Fn) is a high molecular weight glycoprotein that is a major component of the extracellular matrix (ECM) of all connective tissues. This multifunctional protein is known to play a role in several fundamental cell functions, adhesion, growth, differentiation or migration [1]. In bone, Fibronectin is involved in the early stages of osteogenesis [2–4] and has been suggested to be able to nucleate mineralization [5,6]. Fibronectin has not only a prominent functional role in connective tissues but is also capable of interacting with a number of matrix components, including type I collagen [7], glycosaminoglycans [8], osteopontin [9] and itself [1,10,11], what makes it a central support of matrix architecture.

Fibronectin is found under compact form in the plasma [12] and at the cell surface [13]. Both are incorporated in the ECM, where they are found under extended forms, which self-associate into a dense fibrilar network [14]. In vivo, the compact-to-extended transition is partly triggered by cell-applied mechanical forces through cell membrane receptors, the integrins [15,16]. Fibronectin is composed of two nearly identical subunits, each of which is a combination of type I, II and III domains (see Fn structure in Fig. 1). Its compact form is stabilized by inter-subunit ionic interactions between $III_{2–3}$ and $III_{12–14}$ or $I_{1–5}$ domains [17] and Fn extension may be triggered by ionic strength increase [18–21] or upon adsorption onto hydrophilic surfaces [22,23]. This transition would allow the exposure of Fn self-association domains required for

Abbreviations: ECM, extracellular matrix; EDTA, ethylenediamine tetraacetic acid; Fn, Fibronectin; F70, Fibronectin 70 kDa N-terminal fragment; HA, hydroxyapatite; THT, thioflavine T; III_n, nth type III Fn domain; I_n, nth type I Fn domain.

* Corresponding author.
E-mail addresses: delphine.pellenc@bio.u-cergy.fr, d.pellenc@reading.ac.uk (D. Pellenc), olivier.gallet@bio.u-cergy.fr (O. Gallet).
[1] Present address: J.J. Thompson Physical Laboratory, University of Reading, Whiteknights Reading RG6 6AF, UK.

0021-9797/$ – see front matter
doi:10.1016/j.jcis.2005.11.059

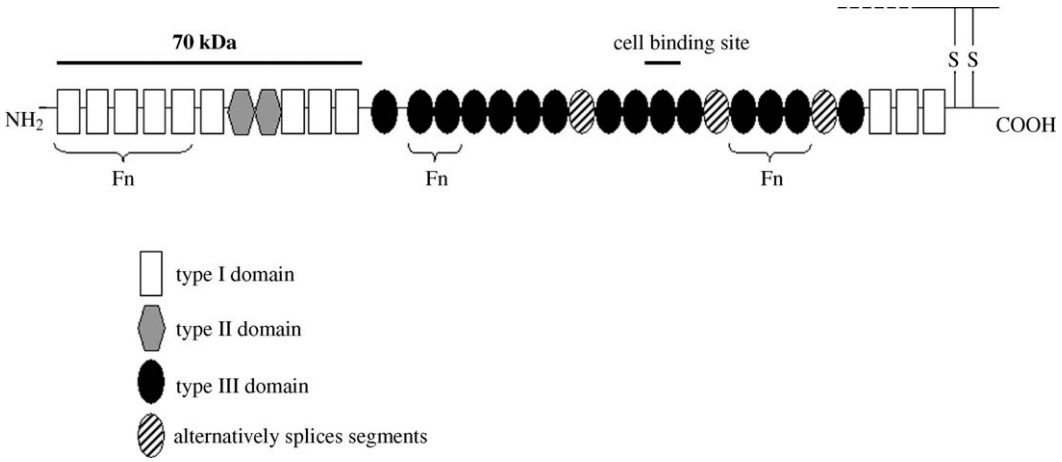

Fig. 1. Fibronectin schematic structure. The combination of type I, II and III domains is represented for one strand of the dimere. Location of cell-binding site, 70 kDa N-terminal fragment and main Fn self-association sites are indicated.

fibril growth but the mechanisms underlying fibril and subsequent network self-assemblies are still under investigation [10,24,25].

Together with the understanding of fundamental processes, Fn self-assembly mechanisms may have relevance in optimizing a biomaterial performance. Calcium phosphate matrices are largely studied as hard tissue implants [26] due to their capacity to establish chemical bonds with the surrounding tissue. Hydroxyapatite (HA) is the major inorganic component of mammalian bones and synthetic HA has been shown to have a high biocompatibility, concerning both cell adhesion [27,28] and plasma protein adsorption [29]. It exhibits large osteoconductive properties in vivo [30,31] and may be used as a model matrix to investigate fundamental mechanisms of bone mineralization [32].

Biomineralization is a physiological process involving crystal formation in living organisms. In addition to regulate cellular functions, bone matrix proteins, the synthesis of which is synchronized in time and location with the mineralization process [33,34], are now known to play a direct role in the mineral nucleation and growth [35–38]. This activity is tightly linked to their structural organization onto the mineral matrix that would provide the confined space and physicochemical local environment needed for the ordered morphology of the crystals.

Investigating not only the adsorption properties of ECM molecules but also their assembling properties at the supramolecular scale on mineral matrices might therefore help the understanding of some mineralization fundamentals. While fibronectin adhesive properties have been extensively used to improve the biocompatibility of hard tissue implants [39–41], little is known about the influence of the mineral surface on the protein assembly. Our purpose here is the investigation of fibronectin supramolecular assembly induced by its adsorption onto a model mineral matrix of hydroxyapatite. We characterize the aggregative structures and the sequence of the assembly and try to decipher responses of this assembly to variations of the physicochemical environment of the protein in order to elucidate the interactions involved in fibronectin adsorption and self-association on HA.

2. Materials and methods

2.1. Hydroxyapatite ceramic disks

Hydroxyapatite powder, synthesized by wet precipitation route, was kindly provided by Pr Eric Champion (SPCTS UMR CNRS 6638, Université de Limoges, France). Hydroxyapatite disks, 13 mm diameter and 3 mm thick, were fabricated by pressing the powder under 80 MPa for 15 s. After compression, disks were sintered for 2 h at 1200 °C. Phase composition was checked with X-ray diffraction. Prior to adsorption experiments, the ceramics disks were immersed for 24 h at 37 °C in the adsorption buffer to allow surface chemical and thermal equilibration.

2.2. Fibronectin purification

Fibronectin was purified from human cryoprecipitated plasma (kind gift from Laboratoire du Fractionnement et des Biotechnologies, Les Ulis, France) according to Poulouin et al. [42]. This purification process has been shown to provide a protein solution exhibiting a purity of about 98% w/w. Fibronectin was stored at 8 °C in 50 mM Tris buffer pH 7.4, containing 1 mM EDTA. Prior to each series of adsorption experiments, fibronectin was filtered through a 0.2 μm sieve to remove large protein aggregates that might have grown in solution.

For cell adhesion experiments, filtration was processed under sterile atmosphere. All the adsorption experiments were carried out at 37 °C and, unless otherwise stated, for 2 h with fibronectin diluted 0.1 g/L in 50 mM Tris buffer pH 7.4.

2.3. Adsorption experiments

To assess the influence of ionic strength on fibronectin surface assembly, different NaCl 50 mM Tris buffers were made, the composition of which is summarized in Table 1. Ionic strengths are calculated for a fibronectin concentration of 0.1 g/L at pH 7.4. The influence of a non-ionic surfactant on fibronectin assembly was assayed using poly-oxyethylensorbitan

Table 1
Adsorption buffer composition. Each buffer contains 50 mM Tris, various amounts of NaCl and is buffered at pH 7.4

Buffer	T50	T50N2	T50N5	T50N15	T50N20	T50N50	T50N150	T50N500
NaCl (mM)	0	2	5	15	20	50	150	500
Ionic strength	0.048	0.050	0.053	0.063	0.068	0.098	0.198	0.548

monolaurate (Tween20®, Sigma-Aldrich, USA). Tween20 was extemporaneously added to fibronectin solutions to a final Fn/Tween20 molar ratio ranging from 0.1 to 100. The highest Tween concentration remains below the surfactant's critical micellar concentration, which is 60 mg/L. The possibility that the adsorption conditions used here may induce fibronectin multimerization in solution was assessed using polyacrylamide gel electrophoresis under non-denaturing and non-reducing conditions. This showed no evidence of fibronectin multimerization when the protein was kept at 37 °C, up to 20 h in each adsorption condition.

2.4. N-terminal 70 kD fibronectin fragment

Adsorption experiments involving the N-terminal domain of the fibronectin were performed using the purified 70-kDa fibronectin N-terminal domain (F70) (Sigma-Aldrich, USA). The fragment was homogeneously added to fibronectin solutions at the beginning of the adsorption experiment. Fibronectin concentration was kept at 0.1 g/L and the Fn/F70 molar ratio ranged from 0.1 to 1.0.

2.5. ELISA assay

The amount of fibronectin adsorbed onto HA samples was quantified using direct ELISA. Ceramic samples were saturated for 1 h at 37 °C in 3% non-fat milk Tris buffer. They were incubated for 1 h at 37 °C with rabbit anti-human plasma fibronectin polyclonal antibody (Sigma F-3648) diluted 1:5000 in saturation buffer and washed three times with the saturation buffer. Samples were then incubated for 1 h at 37 °C with goat anti-rabbit IgG phosphatase alkaline-conjugated antibody (Sigma A3687) diluted 1:15,000 in saturation buffer, and washed three times in Tris buffer. They were finally incubated for 1 h at 37 °C with PNPP diluted 0.3% w/v in diethanolamine. PNPP hydrolysis product was detected spectrophotometrically at 405 nm.

2.6. Fn cell-binding site (cbs) exposure

Fibronectin cell-binding site exposure was estimated by direct ELISA using the same procedure as described above except that the primary antibody was a mouse monoclonal anti-Fn cbs antibody (Chemicon MAB1933) diluted 1:1000, and the secondary one a sheep anti-mouse IgG phosphatase alkaline-conjugated antibody (Sigma A5324) diluted 1:15,000.

2.7. Desorption

Next to the adsorption experiments, ceramics were rinsed with Tris buffer to remove loosely bound fibronectin. They were then immersed for 24 h at 37 °C in 50 mM Tris buffer. The protein amount released in the supernatant was determined by colorimetric protein assay (Biorad protein assay).

2.8. Immunofluorescent staining

In situ detection of the fibronectin coating onto HA ceramics was performed by immunofluorescent staining. Following Fn adsorption, ceramic samples were saturated for 1 h at 37 °C in 3% non-fat milk Tris buffer, prior to immunodetection assay. They were then incubated for 1 h at 37 °C with rabbit anti-human plasma fibronectin polyclonal antibody (Sigma F-3648) diluted 1:1000 in the saturation buffer, washed three times, and incubated for 45 min at room 37 °C with goat anti-rabbit IgG TRITC-conjugated antibody (Sigma T-6778) diluted 1:500 in the saturation buffer, and finally washed 3 times in Tris buffer. Fluorescence images were obtained with bandpass filter centred at 570 nm. All controls for non-specific labeling yielded only background fluorescence.

2.9. Thioflavine T staining

Fibronectin fibril structure was investigated using thioflavine T (Sigma Chemical; St Louis, MO, USA), a non-specific stain for amyloid fibrils with a beta-sheet structure [43]. Thioflavine T (THT) was diluted in Tris buffer at a concentration of 1 mM and then filtered three times through a 0.2 μm sieve. Prior to the adsorption experiments, THT was mixed with Fibronectin to a final Fn:THT molar ratio of 55:1. After supernatant removal and sample gentle wash, fibronectin immunofluorescent staining was performed as described above. Samples were then observed with a fluorescence microscope. Fluorescence images were obtained with bandpass filters centred at 480 and 570 nm to isolate spectrally the THT and TRITC probes respectively.

2.10. Morphological state frequency

From 5 to 20 fields were randomly chosen on each sample, depending on the sample variability. The occurrence frequency of one fibronectin morphological state is expressed as the number of fields presenting this state over the total number of fields observed. The results are then presented as the mean ± s.d. of this frequency over the total number of samples in a given condition. Connected fibrils prevailed over isolated ones in counting these state frequencies so that the total fibril proportion does not contain any duplication.

2.11. Cell adhesion experiments

Cell adhesion assays were performed using MG 63 cells. These cells are derived from osteosarcomic human cells and

able to differentiate into osteoblastic cells under specific conditions. All cell culture products were purchased from Eurobio. Cells were grown in HAM F12 medium complemented with 10% foetal calf serum, 1% penicillin/streptomycin and 1% glutamine. When cells reached 80% confluence, they were released from the substrate by treating with 2 ml of 0.5 g/L trypsin in 0.2 g/L EDTA, diluted in 25 ml complete medium and centrifuged for 5 min at 1200 g. The pellet was resuspended either in complete medium or in serum-free medium for cell adhesion assays. Cells were then seeded on ceramics, which had been previously coated with fibronectin. After 2 h incubation, samples were gently washed with TBS to remove unattached cells. 500 µL MTT, diluted 0.5 mg/mL in HAM F 12 medium, were then added to each well and incubated for 3 h. Reduced MTT was released with addition of 1 ml of isopropanol/HCl 0.1 N and the number of cells was estimated spectrophotometrically at 570 nm. Cell adhesion was expressed as a percentage of the adhesion measured on uncoated HA.

Statistics—all statistical differences between mean values were decided by comparing deviations with a Fischer test and then comparing the means using the appropriate Student t-test. Minimal p-value is indicated in each case.

3. Results

3.1. Four morphological states

Fibronectin adsorption onto HA spontaneously induces its aggregation and fibrillogenesis as shown by immunofluorescent staining (Fig. 2). The different states that are observed are classified into four categories according to their morphological features: Homogeneous Coating, Aggregates, Isolated Fibrils and Connected Fibrils. Homogeneous Coating refers to a state where the fluorescent staining of adsorbed fibronectin presents a uniform intensity, i.e. when none of the other structures is observed (Fig. 2a). This does not mean that the fibronectin coating does not exhibit any particular organization at all, but that, if present, its characteristic scale lies below optical resolution so that we may not differentiate it from a truly uniform distribution. Aggregates are small compact structures, exhibiting irregular shapes. Their larger dimension typically ranges from a few to a few tens of micrometers (Fig. 2b) but bigger aggregates, about 50 µm long, could be observed in few cases. Upon adsorption onto HA, fibronectin also forms elongated fibrilar structures, exhibiting a linear or tortuous shape (Figs. 2c and 2d). Their length ranges from tens to thousands of micrometers on average and may occasionally reach the millimetre (Figs. 2d and 2e). Fibronectin fibrils may be found isolated or connected one to the other. Some fibrils exhibit a marked direction change that could let suppose that two fibrils are linked, but we consider fibrils to be connected only when no less than three branches emerge from what is thus referred to as a node, i.e. only when there was no uncertainty about a connexion (see asterisks in Figs. 2e and 2f). Fibronectin may also display thicker elongated structures that suppose lateral interactions between individual fibrils (see arrows in Figs. 2e and 2g). Ultimately, fibronectin connected fibrils may turn into a dense network of highly ramified structures (Figs. 2g and 2h).

3.2. Time sequence of the assembly

Fibronectin assembly onto hydroxyapatite is a time-dependent process, the sequence of which is presented in Fig. 3. At low bulk concentration (Fig. 3a), fibronectin aggregates appear on the surface within the first five minutes of adsorption and persist over hours, their proportion being unchanged with time. Conversely, almost no fibrils are present at the beginning of adsorption. Their total proportion significantly increases after 30 min but remains about three times lower than the aggregate one. This proportion represents mostly isolated fibrils as the proportion of connected ones stays below 0.1 at all times. Despite changes in morphology, and especially fibril emergence, at this concentration, fibronectin amount on HA does not significantly change with time, as shown by direct Fn ELISA assay on ceramic samples (Fig. 4a).

3.3. Effect of the bulk concentration on the assembly

Fibronectin concentration in the bulk has significant impact on the protein surface assembly. Increasing Fn bulk concentration from 0.01 to 0.1 g/L results in a twofold increase in isolated fibrils (Fig. 3b). A second increase in concentration displaces the effect towards connected fibrils (Fig. 3c). In this latter case, the increase is observed at short times but results in the same total fibril proportion than at 0.1 g/L after 15 h adsorption, suggesting an acceleration of the process rather than further fibril creation. Fibronectin concentration in the bulk has an opposite effect on aggregates, its increase significantly decreasing their proportion. Surprisingly, when probing fibronectin quantity, the higher the concentration and the longer the adsorption time, the lower the amount of the protein on HA ceramics (Fig. 3a). Fibronectin is detected using direct ELISA, the procedure of which implies several hours of incubation in Tris buffers. Low detected amounts of fibronectin could thus be due either to lower adsorption or to a higher desorption during the assay. To settle the question we assayed fibronectin desorption from HA samples with respect to the adsorption time and bulk concentration. This revealed a fourfold higher desorption for 1 g/L–15 h adsorption, compared with the other time and concentration conditions (Fig. 5). Between these, no significant differences are observed between desorbed quantities, while there are differences in the amount detected on the surfaces of HA samples (Fig. 4a). If desorption is involved, it might therefore not be the only reason for low fibronectin detection, and differences during the adsorption step might be implicated as well. The differences observed may also result from conformational changes of fibronectin that may impair the binding of the antibody and thus bias the amount of fibronectin detected on HA.

One should note here that, despite desorption, since immunofluorescence and ELISA are very similar methods, as far as incubation times, buffer composition, and antibody type are concerned, the amount detected by the latter remains rel-

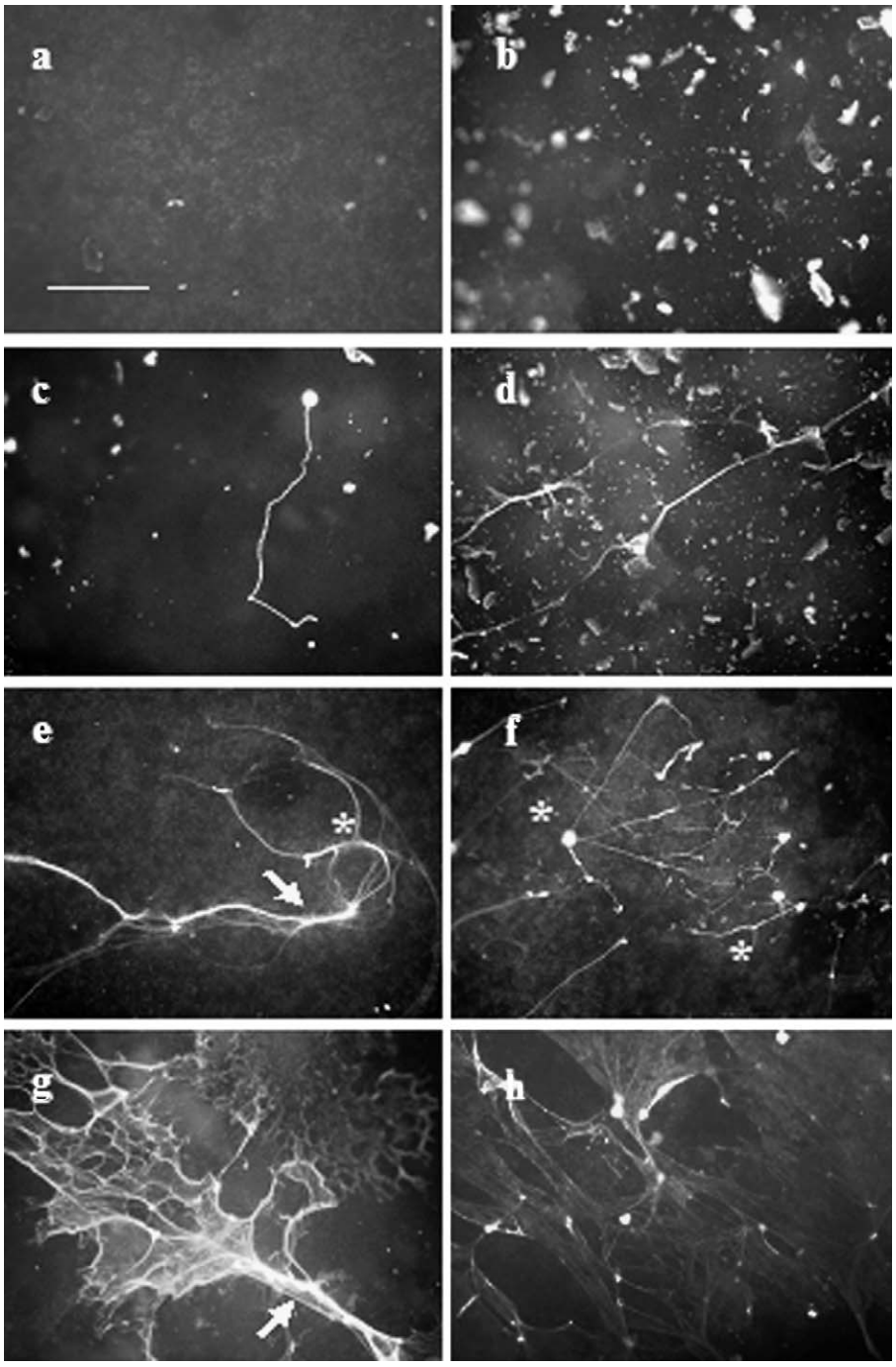

Fig. 2. Fibronectin morphological states on hydroxyapatite. Fibronectin was observed by immunofluorescent staining following adsorption of the protein diluted 1 g/L in T50 buffer. In this condition, fibronectin exhibits four distinct morphologies: homogeneous coating (a), aggregates (b), isolated (c, d) or connected (e, f) fibrils. In some cases, fibronectin fibrils are connected into large clusters covering the surface (g, h). Asterisks on (e) and (f) show examples of nodes between connected fibrils. The arrows on (e) and (g) indicate thicker structures were lateral interactions between individual fibrils are thought to occur. Note that both isolated and connected fibrils often coexist with aggregates (d, f, h). The scale is the same on all images and the white bar on (a) represents 100 μm.

evant when discussing the former. In order to examine a possible correlation between fibronectin supramolecular organization and conformation, we investigated the accessibility of the fibronectin cell-binding site (cbs) with respect to the adsorption time and concentration but could not find any significant difference among adsorption conditions (Fig. 4b). Due to a high variability of the staining, no significant change is observed either when relating the cbs exposure to the total fibronectin amount, as shown by the ratio between both detection levels in each condition (not shown).

3.4. MG63 cell adhesion

Fibronectin layer morphology might directly influence its function and we assessed this relationship by evaluating MG63 cell adhesion with respect to Fn adsorption conditions. MG63

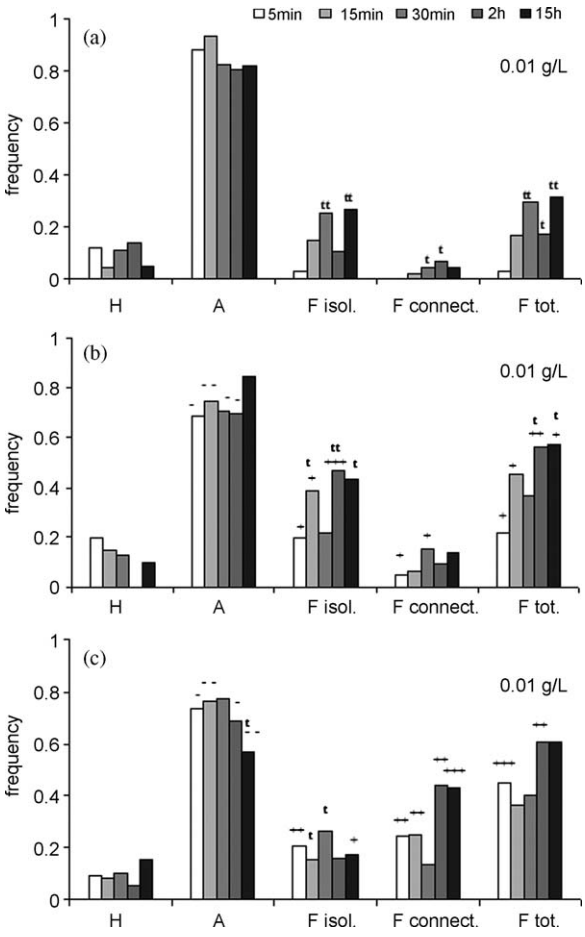

Fig. 3. Time-sequence of fibronectin assembly on HA with respect to bulk concentration. The occurrence frequency of each of the four morphological states (see illustrations in Fig. 1) is followed between 5 min and 15 h at fibronectin bulk concentration (a) 0.01 g/L; (b) 0.1 g/L; (c) 1 g/L. Frequencies are calculated from immunofluorescent images as described in Section 2. H, homogeneous coating; A, aggregates; F isol., isolated fibrils; F connect., connected fibrils and F tot., total fibrils. Results are means over 9 samples. s.d. bars have been omitted for clarity. For each concentration and type of structure we tested the significance of the time evolution against the time 5 min, t: $p < 0.05$; tt: $p < 0.01$. Statistical significance of the bulk concentration increase is tested against the concentration 0.01 g/L: We indicated: +, $p < 0.05$; ++, $p < 0.01$; +++, $p < 0.001$ when the frequency was found higher than that at 0.01 g/L, or -, $p < 0.05$; - -, $p < 0.01$ when it was found lower.

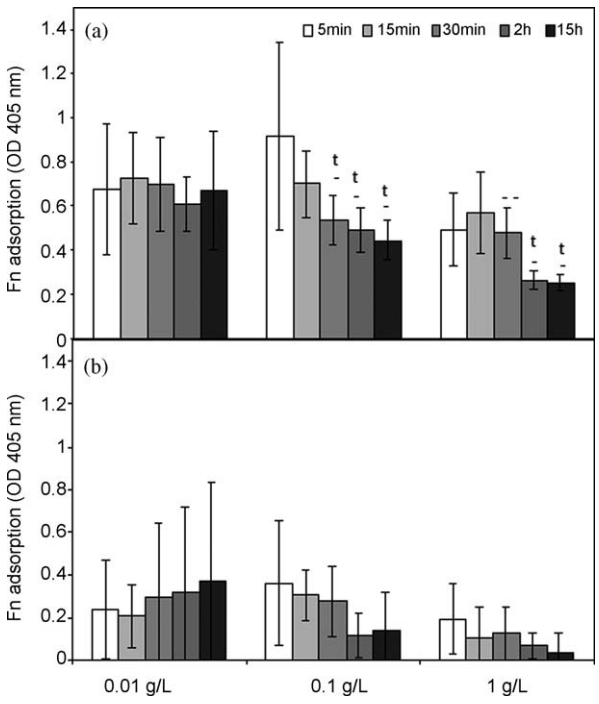

Fig. 4. Time evolution of fibronectin total adsorption and cell binding site (cbs) exposure on HA with respect to bulk concentration. Fibronectin was let adsorb onto hydroxyapatite for 2 h in T50 buffer. We quantified (a) Fn adsorption by direct ELISA using a polyclonal anti-Fn antibody and (b) Fn cell binding site (Fn-CBS) exposure using a monoclonal anti Fn-CBS antibody. This was done for three different Fn bulk concentrations 0.01, 0.1 and 1 g/L from 5 min to 15 h. Results are means over 4 samples. For each concentration we tested the significance of the time evolution against the time 5 min, t: $p < 0.05$. Statistical significance of the bulk concentration increase is tested against the concentration 0.01 g/L: -, $p < 0.05$; - -, $p < 0.01$.

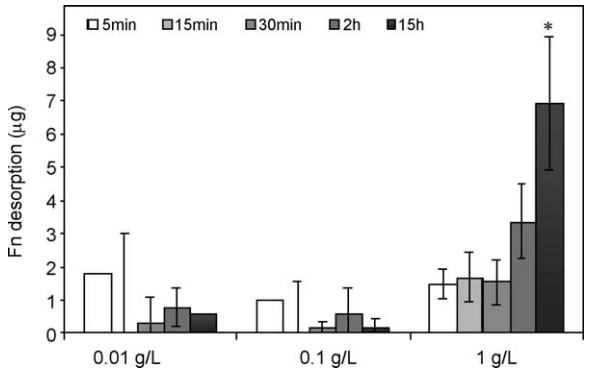

Fig. 5. Fibronectin desorption from HA with respect to Fn bulk concentration and adsorption duration. Following Fn adsorption at 0.01, 0.1 or 1 g/L from 5 min to 15 h, HA samples were immersed for 24 h in T50 buffer. Fn desorption was then deduced from protein amount detected in the supernatants. Results are mean over 3 samples. Significant difference with desorption at 5 min: *, $p < 0.05$.

cell adhesion is only poorly affected by Fn concentration or adsorption time (Fig. 6). Except a higher adhesion after 5 min adsorption of 0.01 g/L Fn, compared to other conditions, no other significant evolution is observed. Consistent with the variability in Fn cell-binding site exposure (Fig. 4b), we found a high variability of cell adhesion with respect to Fn bulk concentration and adsorption duration, so that we could not show any significant correlation with fibronectin amount or morphological state. MG63 cell adhesion on uncoated Hydroxyapatite is already very high, compared to that on tissue-culture polystyrene for instance. If the fibronectin layer on HA does not completely cover the surface, as suggested by immunofluorescence images, overall cell adhesion may actually mostly reflects adhesion on uncoated HA surface surrounding Fn. However, these preliminary results would require further investigations.

3.5. Ionic strength

As electrostatic interactions may influence both fibronectin tertiary structure and binding to the HA surface, we investigated the effect of varying the ionic strength in the bulk on fibronectin assembly on HA. Fig. 7 illustrates fibronectin morphological structures observed for three different ionic strengths. At the

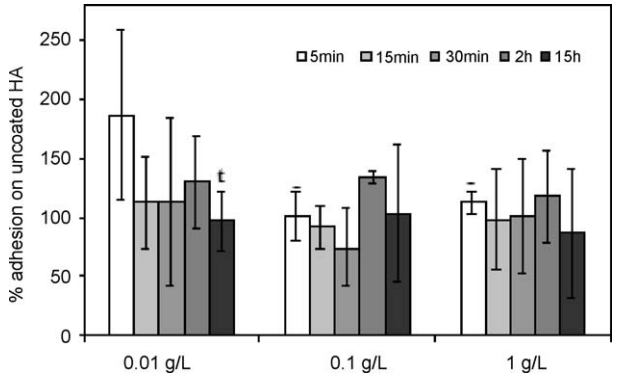

Fig. 6. MG63 cell adhesion on Fn-coated HA with respect to Fn bulk concentration during adsorption. MG63 cells adhered for 2 h on HA samples previously coated with 0.01, 0.1 or 1 g/L Fn during 5 min to 15 h. Cell adhesion was evaluated using MTT assay and expressed in percentage of adhesion on uncoated HA. Significant difference with 5 min condition: t, $p < 0.05$; with 0.01 g/L condition: -, $p < 0.05$.

lowest value (T50, $I = 0.048$), fibronectin exhibits both fibrils and aggregates, as described previously. At higher value (T50N20, $I = 0.068$), fibronectin exhibits only aggregates disseminated all over the surface and with quite regular shape and size. At high ionic strength (T50N500, $I = 0.548$), both morphological states are found again. Note that in this condition, fibrils are similar in aspect to those observed at low ionic strength. The frequency of each morphological state over a whole range of ionic strength values is presented in Fig. 8. This shows biphasic behaviours of aggregate and fibril proportion with respect to increasing ionic strength, i.e. an initial increase in aggregate and decrease in fibril proportion, the latter completely disappearing between $I = 0.063$ and 0.198, followed by a reversal of the effect, i.e. a decrease in aggregate and increase in fibril proportion. The ionic strength increase is correlated with an increase in fibronectin adsorption (that might also be due to a decrease in desorption during detection assay, as seen before), which reaches a plateau value beyond $I = 0.068$ (Fig. 9a), where there is a rapid increase in cbs exposure (Fig. 9b).

3.6. Non-ionic surfactant

Further investigation of the interactions at work in fibronectin assembly on HA was carried out by examining the effect of adding Tween20, a non-ionic surfactant, in three different ionic strength adsorption buffers. Without salt, for an equimolar Tween/Fn ratio, fibronectin fibril morphology is similar to that observed without Tween; while a hundred times higher Tween/Fn molar ratio results in the complete disappearance of fibronectin fibrils on HA and only very small aggregates are observed (Fig. 10). Both morphological states evolve in a slightly different way with respect to Tween content, as aggregate proportion suddenly increases at low tween content, while total fibril proportion seems to be more gradually lowered with increasing Tween (Fig. 11a). At intermediate ionic strength value, Tween has no effect either on aggregate aspect (Fig. 10) or on its proportion (Fig. 11c). At high ionic strength, the presence of a non-ionic surfactant does not change fibril proportion but increases aggregate one in a sudden fashion, in a way similar to the effect observed at low ionic strength. In general, increasing Tween content leads to an in increase in fi-

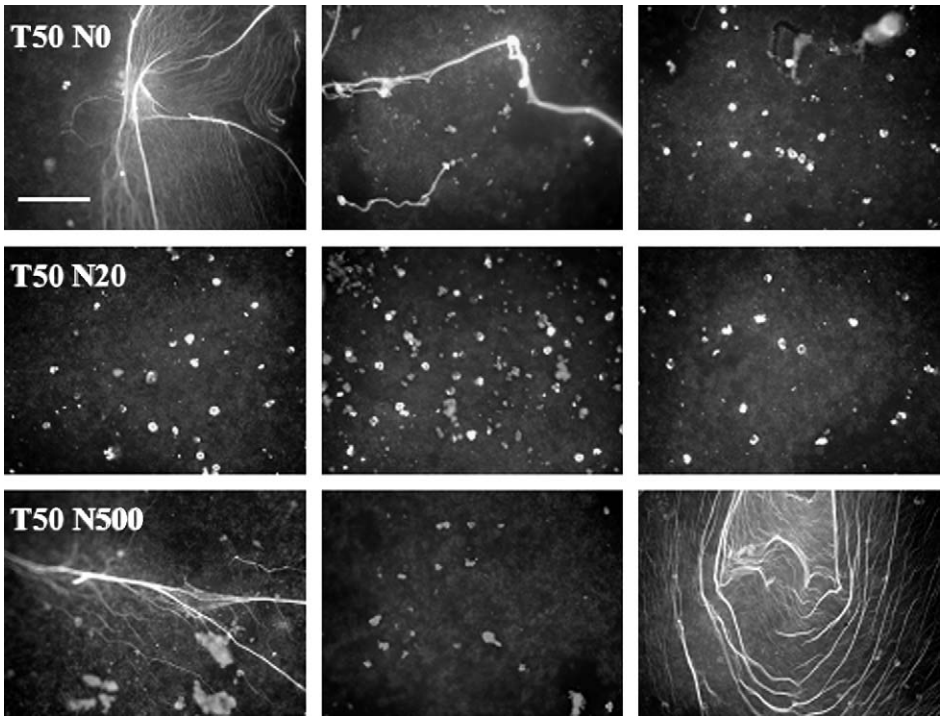

Fig. 7. Ionic strength influence on fibronectin assembly on HA Fibronectin, diluted 0.1 g/L in T50Nx (Tris 50 mM, NaCl x mM, pH 7.4) buffers, adsorbed on HA samples for 2 h at 37 °C. Each row presents 3 illustrations of the structures observed in each ionic strength condition. The scale is the same on all images and the white bar on top-left picture represents 100 μm.

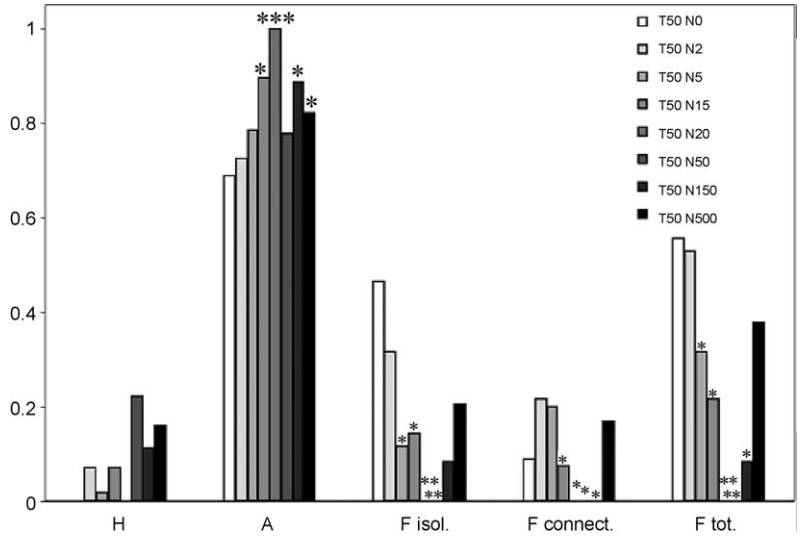

Fig. 8. Fibronectin morphological state occurrence on HA with respect to the ionic strength in the bulk. Fibronectin, diluted 0.1 g/L in T50Nx (Tris 50 mM, NaCl x mM, pH 7.4) buffers, adsorbed on HA samples for 2 h at 37 °C. Fn state abbreviations are the same as in Fig. 3. Results are means over 7 samples; s.d. have been omitted for clarity. Significant difference with respect to T50 condition *, $p < 0.05$; **, $p < 0.01$; ***, $p < 0.001$.

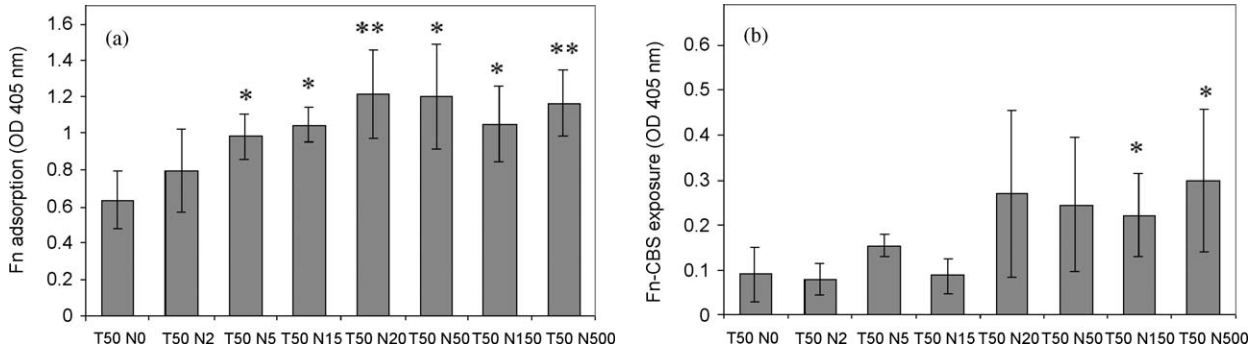

Fig. 9. Ionic strength effect on fibronectin adsorption and cbs exposure on HA Fibronectin, diluted 0.1 g/L in T50Nx (Tris 50 mM, NaCl x mM, pH 7.4) buffers, adsorbed on HA samples for 2 h at 37 °C. Fn total adsorption and cbs exposure are quantified using direct ELISA. Results are means over 4 samples. Significant difference with respect to T50 condition: *, $p < 0.05$; **, $p < 0.005$.

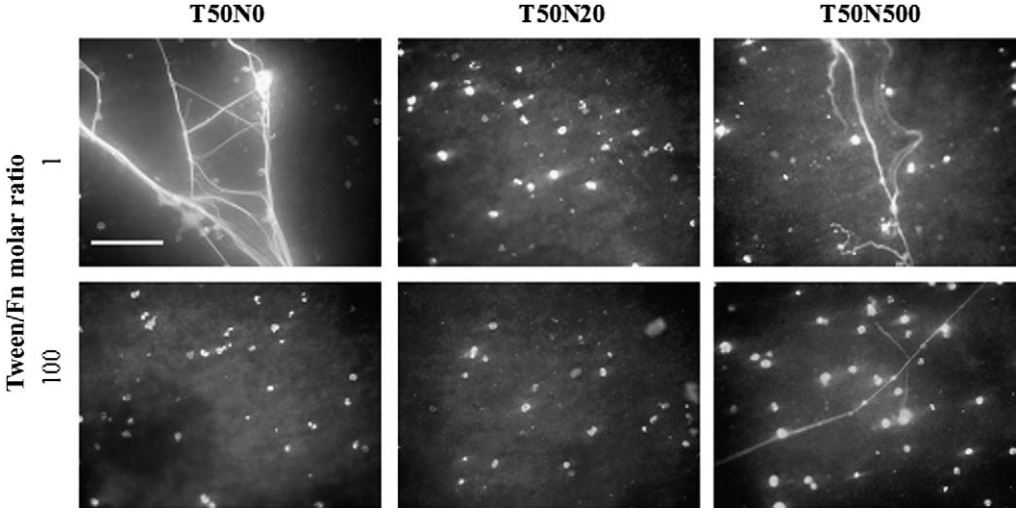

Fig. 10. Ionic strength and non-ionic surfactant influences on fibronectin assembly on HA. Fibronectin, diluted 0.1 g/L in T50Nx (Tris 50 mM, NaCl x mM, pH 7.4) buffers, containing Tween20 to a final Tween/Fn molar ratio 1 or 100, adsorbed on HA samples for 2 h at 37 °C.

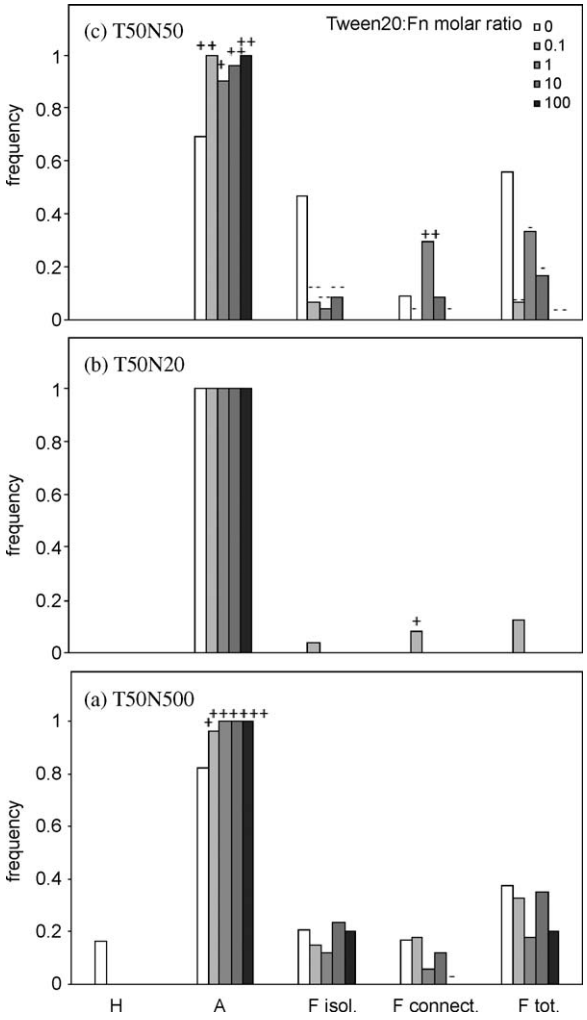

Fig. 11. Effect of a non-ionic surfactant on fibronectin morphological state occurrence on HA with respect to the ionic strength in the bulk Tween20 was added to each adsorption buffer (a) T50N0, (b) T50N20 or (c) T50N500 to a final Tween/Fn molar ratio ranging from 0 to 100. Fn state abbreviations are the same as in Fig. 3. Results are means over 3 samples; s.d. have been omitted for clarity. Significant difference with respect to the same ionic strength condition without Tween: higher frequency +, $p < 0.05$; ++, $p < 0.01$; +++, $p < 0.001$; lower frequency -, $p < 0.05$; - -, $p < 0.01$; - - -, $p < 0.001$.

bronectin adsorption (Fig. 12) and the lower the ionic strength the stronger the effect. All the ionic strengths generate the same fibronectin amount at the highest Tween content so that Tween and ionic strength appear to have the same promoting effect on fibronectin adsorption.

3.7. Fn N-terminal domain

Fibronectin self-association is known to rely on interactions between specific domains of the protein among which the N-terminal domain is the most prominent [44,45]. We examined the inhibitive potential of a fibronectin 70 kD N-terminal fragment (F70) on fibronectin self-assembly onto HA. Whatever its amount, the presence of F70 does not affect the aggregate proportion but significantly reduces the isolated fibril proportion (Fig. 13). It does not have much effect on connected ones and

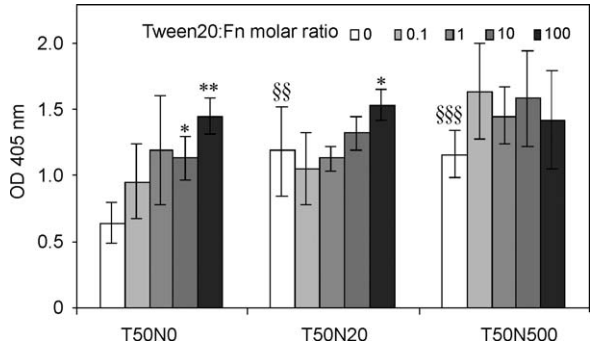

Fig. 12. Effect of a non-ionic surfactant on fibronectin adsorption onto hydroxyapatite with respect to the ionic strength in the bulk Fn total adsorption is quantified using direct ELISA. Results are means over 3 samples. Significant difference with no Tween condition *, $p < 0.05$; **, $p < 0.01$ and with T50 condition, at the same Tween content §§, $p < 0.01$; §§§, $p < 0.001$.

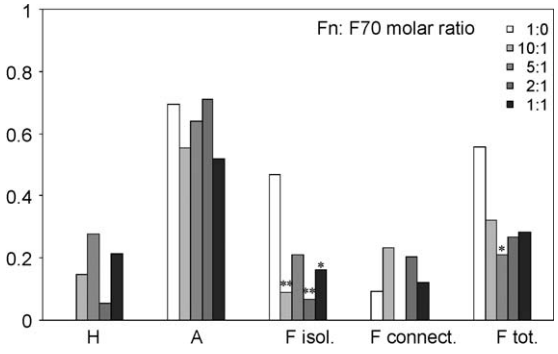

Fig. 13. 70 kDa N-terminal Fn fragment (F70) inhibition assay of fibronectin assembly. F70 was added to 0.1 g/L Fn to a final Fn:F70 molar ratio ranging from 10 to 1. Significant difference with the frequency without F70 **, $p > 0.001$; *, $p > 0.01$.

the decrease in total fibril proportion appear to be not significant.

3.8. Thioflavine T staining of amyloid-like structures

Amyloid fibrils are protein aggregative structures involved in many neurodegenerative diseases [46]. As fibronectin is supposed to have an amyloidogenic potential [47] and as amyloid fibrils may be surface-induced [48], we wondered whether our adsorption-induced fibronectin structures exhibited amyloid-like properties and probed them using thioflavine T (THT), a non-specific fluorescent dye of amyloid structures [49,50]. We observed THT staining, with respect to adsorption time and bulk concentration. The results are exemplified for Fn 1 g/L on Fig. 14. In this condition, except at short time (Fig. 14a), most fibronectin aggregates are THT-stained (Figs. 14b, 14c, and 14e). THT incorporation into fibronectin fibrils appears to be more variable as there may be stained or unstained fibrils in the same adsorption condition (Figs. 14d and 14e). At lower bulk concentration, the staining is overall less significant and as much variable (not shown) and we are not able to decipher any correlation of the staining with the adsorption time, or fibronectin morphological state. Fibronectin amyloid-like structures seem to form on HA, but this does not appear to be the main mechanism for fibrils assembly.

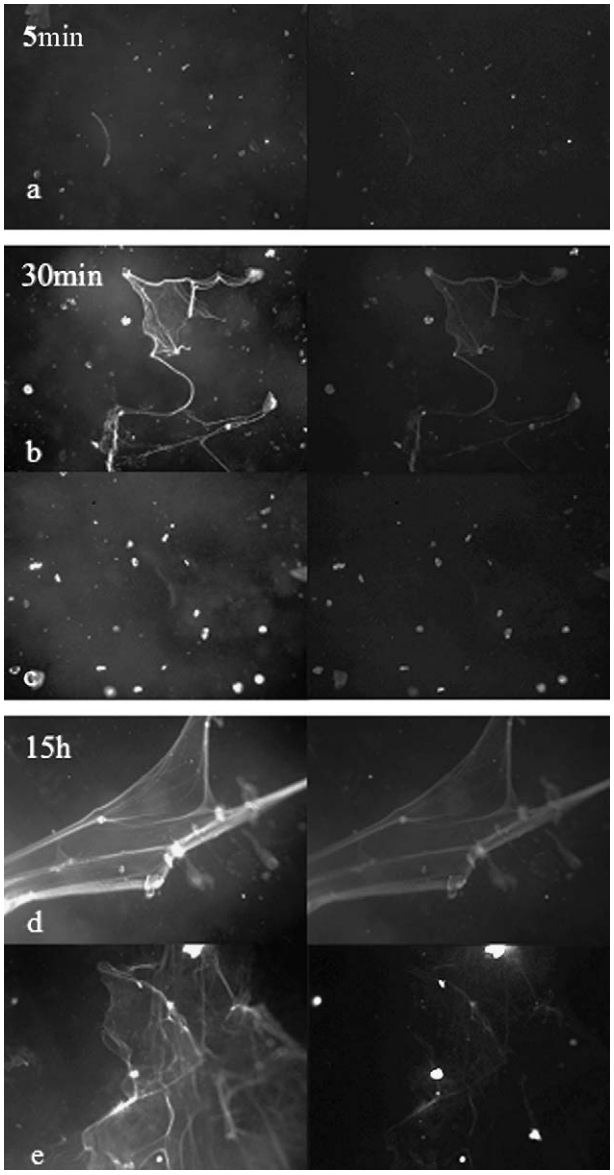

Fig. 14. Amyloid-like structure in fibronectin aggregates and fibrils on HA 1 g/L fibronectin adsorbed with thioflavine T in T50 buffer. Right panel: THT staining; left panel: immunofluorescent staining. In this condition, at short time, aggregates do not incorporate THT (a) while they are often stained at longer times (b, c, e). In general, fibrils exhibit a quite strong THT staining (b, d) while some connected ones are not stained at all (e).

4. Discussion

At low bulk concentration, fibronectin aggregates appear within minutes on hydroxyapatite surface, while fibril proportion increases rather slowly with time. This delay between both structures emergence raises the question whether aggregates only precede or also nucleate fibril formation, i.e. whether both morphological states belong to the same organization path. If fibrils were directly formed from aggregates, the persistence of the latter with time, at low bulk concentration, would imply a simultaneous increase in fibronectin amount. This is not supported by our results (Fig. 4a). Alternatively, fibrils could be formed from the reorganization of molecules adsorbed within minutes but that are not aggregated, while aggregates would remain amorphous structures. In contradiction with this view, at high bulk concentration, the faster fibril formation is concomitant to a decrease in aggregate proportion with time. This decrease seems however unlikely to occur out of desorption, since there is no reason this would not be the case at low bulk concentration. Hence, our data suggest that the actual scenario of fibronectin fibrillation might be more complex. The concentration-induced increase in fibril proportion is mainly due to the appearance of connected fibrils. Except in few cases where the network covers large surface areas, fibrils are connected into small clusters laying separate one from another. This indicates that connexion is more likely to occur through a branching process, i.e. fibrils are grown from the same origin (node), rather than through joining of independently grown fibrils, which would require a high fibril surface coverage for meeting to occur. The decrease in aggregate proportion might actually be directly correlated to the appearance of nodes, the former being the origin of the latter. Consistent with this view, we may observe that aggregates are often—but not exclusively—positioned at the intersection of fibronectin fibrils (see Figs. 2f and 2g) when both are present. Thus, one possibility could be that a different type of aggregates forms at higher bulk concentration and is able to nucleate fibrils (see Fig. 15a).

Our discontinuous time observation does not allow ascertaining that fibril-nucleating aggregates would be favoured at higher concentration, but several data in the literature point out that such mechanisms might be at work in fibronectin assembly onto hydroxyapatite. Our results indicate that aggregates that form at low and high bulk concentration might be different in nature, and this is likely to be related to surface coverage. It is known that most proteins undergo structural rearrangement upon adsorption [51,52]. Out of steric hindrance, the extent of these surface-induced denaturations is reduced as the bulk concentration, and hence the surface coverage, increase [53–55]. Incidentally, at high bulk concentration, the lower protein/surface contact area results in a higher degree of desorption [56], in agreement with our observed desorption during the detection assay. Simple excluded volume effects might therefore explain how different fibronectin conformations would arise onto HA with respect to adsorption bulk concentration. Though the underlying molecular mechanism would require further investigation, we may speculate that the ‘fibril-competent’ form at higher bulk concentration might be linked to a higher flexibility of the molecules weakly bound to the substrate. At low surface coverage, fibronectin exhibits a higher stiffness, when compared to high surface coverage, as shown by force microscopy studies [57]. This flexibility at high bulk concentration might allow the reorganization of fibronectin aggregates that is required for fibril growth to occur.

At low ionic strength value, fibronectin is under a compact soluble form that is stabilized by inter-subunit electrostatic interactions [17]. Moreover, at pH 7.4, fibronectin, which is an acidic protein with $pH_i = 5.5$, has an overall negative charge. In these conditions, repulsive interactions between Fn molecules

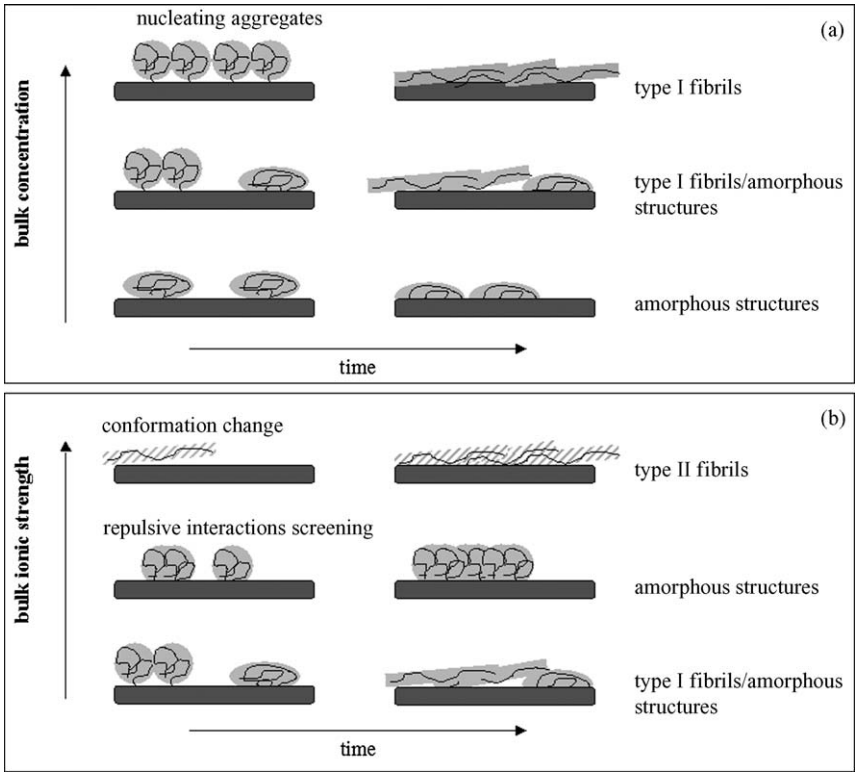

Fig. 15. Hypothetic model of fibronectin assembly on HA with respect to (a) bulk concentration and (b) ionic strength (see Section 4).

are therefore predominant and, despite structural rearrangement that may follow, the initial adsorbing form is rather compact.

Increasing the ionic strength will first decrease the repulsion between adsorbed molecules and incoming ones from the bulk, as well as repulsion between adsorbed molecules themselves. This might respectively explain the observed increases in surface aggregation and fibronectin adsorption (see Fig. 15b). This concomitantly leads to the complete disappearance of fibronectin fibrils. As fibronectin aggregation is a very fast process, we conjecture that the aggregates, which are favoured in this case, are amorphous ones, since one might expect they would have lead to fibril growth after 2 h adsorption if they were nucleating ones. We may not exclude the hypothesis though, that these associated forms may need longer time for fibrils to grow, a step that would then only be delayed.

A higher ionic strength does not further enhance fibronectin adsorption but increases again the fibril proportion. Increasing ionic strength triggers Fn transition from compact to extended form [19–21,58] with minimal changes in intra-subunit tertiary structure [21]. The Fn domains that would be involved in the compact conformation of the protein [17,59] are also predictably involved in Fn–Fn intermolecular association [44,45]. Above 50 mM NaCl, Fibronectin fibrillogenesis onto HA would therefore be favoured by extension of the molecules in the bulk, so that it would adsorb under a conformation where self-association domains might already be exposed (see Fig. 15b). Consistent with this view, Pernodet et al. observed the induction of fibronectin fibrillogenesis upon adsorption onto charged surfaces. They discuss their observation in terms of bonding between the surface and Fn charged domains implicated in the compact form, thereby allowing Fn arms extension and adsorption under a fibril-competent form [24]. Fn cell-binding site is situated in the central region of the protein (see Fig. 1). Its exposure increase at high ionic strengths tends to confirm the salt-induced Fn arms extension, but also implies the fibrils formed on HA at low and high ionic strengths have different structures. Consistent with this idea, the addition of a non-ionic surfactant alters fibronectin fibrils only when they are formed at low ionic strength.

If repulsive interactions are certainly involved in Fn/Fn interactions, interactions between Fn and HA are less clear. The addition of Tween 20 has the exact opposite effect to what could be expected if hydrophobic interactions between Fn and HA were at work—i.e. no effect or a decrease in adsorption out of competitive adsorption [60,61]. In addition to favouring Fn adsorption, the presence of a surfactant also promotes its aggregation. Though the exact mechanisms are not fully understood, some authors tend to think that non-ionic surfactants might promote protein unfolding through the penetration of their hydrophobic tail into the apolar region of the protein, thereby exposing hydrophobic patches and promoting either surface/protein [62] or protein/protein hydrophobic interactions [63]. A recent study even suggests that the non-ionic surfactant-induced inhibition of protein aggregation might be linked to the stabilization of small soluble aggregates, preventing further growth, rather than to a complete inhibition of protein association [64]. Hydrophobic regions have been identified inside [65,66] and between [67,68] Fn domains. These regions might underlie Fn interactions with the hydrophobic tail of the surfactant. The observed increase in fibronectin adsorption might

be linked either to a direct promotion of protein/surface interactions, or, to surfactant-induced aggregation in the bulk and direct deposition of the aggregates and, if present, Fn/Tween interactions remain to be elucidated.

Taken together, our results indicate that there might be various aggregated and fibrilar fibronectin structures formed onto HA (see recapitulation in Fig. 15), a feature shared by several proteins [69–71]. Varying the adsorption conditions impairs not only Fn conformation and Fn/Fn interactions in the bulk, but also Fn/Fn interactions on the surface, Fn/HA binding and ultimately HA-induced Fn conformational change, all balancing each other. Preliminary experiments, performed in our laboratory on several biomaterials, showed a strong material dependency of fibronectin adsorption-induced supramolecular assembly, what tends to confirm that the observed behaviours mainly result from the interaction with the hydroxyapatite surface. While the present paper suggests some mechanisms that may be involved, finding out the exact fibronectin surface assembly pathways requires further study. The high variability in cbs exposure, THT staining and cell response to fibronectin fibrils and aggregates with respect to time and concentration suggests moreover that different Fn association mechanisms could take place simultaneously.

Ultimately, fibronectin organization is known to influence cell behaviour and the elucidation of the functional differences between fibronectin states requires further investigation as this could yield insights for the creation of new bone biomaterials.

References

[1] R. Pankov, K.M. Yamada, J. Cell Sci. 115 (2002) 3861.
[2] R.K. Globus, S.B. Doty, J.C. Lull, E. Holmuhamedov, M.J. Humphries, C.H. Damsky, J. Cell Sci. 111 (1998) 1385.
[3] A.M. Moursi, C.H. Damsky, R.K. Globus, J. Cell Sci. 110 (1997) 2187.
[4] A.M. Moursi, C.H. Damsky, D. Zimmerman, J. Lull, R.K. Globus, S.B. Doty, S.I. Aota, J. Cell Sci. 109 (1996) 1369.
[5] G. Daculsi, P. Pilet, M. Cottrel, G. Guicheux, J. Biomed. Mater. Res. 47 (1999) 228.
[6] D. Couchourel, C. Escoffier, R. Rohanizadeh, S. Bohic, G. Daculsi, Y. Fortun, M. Padrines, J. Inorg. Chem. 73 (1999) 129.
[7] K.C. Ingham, S.A. Brew, M. Migliorini, Arch. Biochem. Biophys. 407 (2002) 217.
[8] S.C. Stamatoglou, J.M. Keller, Biochim. Biophys. Acta 719 (1982) 90.
[9] C.M. Giachelli, S. Steitz, Matrix Biol. 19 (2000) 615.
[10] G. Baneyx, V. Vogel, Proc. Natl. Acad. Sci. USA 96 (1999) 12518.
[11] M.A. Chernousov, M.L. Metsis, V.E. Koteliansky, FEBS Lett. 183 (1985) 365.
[12] M. Rocco, O. Aresu, L. Zardi, FEBS Lett. 178 (1984) 327.
[13] G. Baneyx, L. Baugh, V. Vogel, Proc. Natl. Acad. Sci. 99 (2002) 5139.
[14] D.M. Peters, L.M. Portz, J. Fullenwider, D.F. Mosher, J. Cell Biol. 111 (1990) 249.
[15] I.F. Wierzbicka-Patynowski, J.E. Schwarzbauer, J. Cell Sci. 116 (2003) 3269.
[16] G. Baneyx, L. Baugh, V. Vogel, Proc. Natl. Acad. Sci. 98 (2001) 14464.
[17] K.J. Johnson, H. Sage, G. Briscoe, H.P. Erickson, J. Biol. Chem. 274 (1999) 15473.
[18] H.P. Erickson, N.A. Carrell, J. Biol. Chem. 258 (1983) 14539.
[19] N.M. Tooney, M.W. Mosesson, D.L. Amrani, J. Cell Biol. 97 (1983) 1686.
[20] E.C. Williams, P.A. Janmey, J.D. Ferry, D.F. Mosher, J. Biol. Chem. 257 (1982) 14973.
[21] M.J. Benecky, R.W. Wine, C.G. Kolvenbach, M.W. Mosesson, Biochemistry 30 (1991) 4298.
[22] L. Baugh, V. Vogel, J. Biomed. Mater. Res. A 69 (2004) 525.
[23] M. Bergkvist, J. Carlsson, S. Oscarsson, J. Biomed. Mater. Res. A 64 (2003) 349.
[24] N. Pernodet, M. Rafailovich, J. Sokolov, D. Xu, N.-L. Yang, K. McLeod, J. Biomed. Mater. Res. 64 (2003) 684.
[25] J.E. Schwarzbauer, J.L. Sechler, Curr. Opin. Cell Biol. 11 (1999) 622.
[26] M. Vallet-Regí, J.M. González-Calbet, Prog. Solid State Chem. 32 (2004) 1.
[27] K. Kilpadi, P.-L. Chang, S. Bellis, J. Biomed. Mater. Res. 55 (2001) 258.
[28] T. Suzuki, M. Hukkanen, R. Ohashi, Y. Yokogawa, K. Nishizawa, F. Nagata, L. Buttery, J. Polak, J. Biosci. Bioeng. 89 (2000) 18.
[29] A. Rosengren, E. Pavlovic, S. Oscarsson, A. Krajewski, A. Ravaglioli, A. Piancastelli, Biomaterials 23 (2002) 1237.
[30] H. Yuan, Z. Yang, J. deBruijn, K. de Groot, X. Zhang, Biomaterials 22 (2001) 2617.
[31] U. Ripamonti, Biomaterials 17 (1996) 31.
[32] S.G. Rees, D.T. Hughes Wassell, R.J. Waddington, G. Embery, Biochim. Biophys. Acta 1568 (2001) 118.
[33] B. Sommer, M. Bickel, W. Hofstetter, A. Wetterwald, Bone 19 (1996) 371.
[34] K.L. Sodek, J.H. Tupy, J. Sodek, M.D. Grynpas, Bone 26 (2000) 189.
[35] G.K. Hunter, Curr. Opin. Solid State Mater. Sci. 1 (1996) 430.
[36] G.K. Hunter, V. Hauschka, A.R. Poole, L.C. Rosenberg, H.A. Goldberg, Biochem. J. 317 (1996) 59.
[37] F.J.G. Cuisinier, Curr. Opin. Solid State Mater. Sci. 1 (1996) 436.
[38] J. Kirkham, S.J. Brookes, R.C. Shore, S.R. Wood, D.A. Smith, J. Zhang, H. Chen, C. Robinson, Curr. Opin. Colloid Interface Sci. 7 (2002) 124.
[39] T. Matsuura, R. Hosokawa, K. Okamoto, T. Kimoto, Y. Akagawa, Biomaterials 21 (2000) 1121.
[40] I. Degasne, M.F. Baslé, V. Demais, G. Huré, M. Lesourd, B. Grolleau, L. Mercier, D. Chappard, Calcif. Tissue Int. 64 (1999) 499.
[41] C.D. McFarland, S. Mayer, C. Scotchford, B.A. Dalton, J.G. Steele, S. Downes, J. Biomed. Mater Res. 44 (1999) 1.
[42] L. Poulouin, O. Gallet, M. Rouahi, J.M. Imhoff, Protein Expr. Purif. 17 (1999) 146.
[43] H. LeVine III, Protein Sci. 2 (1993) 404.
[44] H. Bultmann, A.J. Santas, D.M.P. Peters, J. Biol. Chem. 273 (1998) 2601.
[45] K.M. Aguirre, R.J. McCormick, J.E. Schwarzbauer, J. Biol. Chem. 269 (1994) 27863.
[46] M. Stefani, C.M. Dobson, J. Mol. Med. 81 (2003) 678.
[47] S.V. Litvinovich, S.A. Brew, S. Aota, S.K. Akiyama, C. Haudenschild, K.C. Ingham, J. Mol. Biol. 280 (1998) 245.
[48] M. Zhu, P.O. Souillac, C. Ionescu-Zanetti, S.A. Carter, A.L. Fink, J. Biol. Chem. 277 (2002) 50914.
[49] M.R. Krebs, E.H. Bromley, A.M. Donald, J. Struct. Biol. 149 (2005) 30.
[50] M.R. Nilsson, Methods 34 (2004) 151.
[51] M.F.M. Engel, C.P.M. Van Mierlo, A.J.W.G. Visser, J. Biol. Chem. 277 (2002) 10922.
[52] J.S. Sharp, J.A. Forrest, R.A. Jones, Biochemistry 41 (2002) 15810.
[53] J. Kim, G.A. Somorjai, J. Am. Chem. Soc. 125 (2003) 3150.
[54] A. Kondo, H. Fukuda, J. Colloid Interface Sci. 198 (1998) 34.
[55] A. Kondo, J. Mihara, A. Kondo, J. Colloid Interface Sci. 177 (1996) 214.
[56] C.R. Wittmer, P.R. Van Tassel, J. Colloids Surf. B: Biointerfaces 41 (2005) 103.
[57] P.Y. Meadows, G.C. Walker, Langmuir 21 (2005) 4096.
[58] M. Rocco, M. Carson, R. Hantgan, J. Biol. Chem. 258 (1983) 14545.
[59] G.A. Homandberg, J.W. Erickson, Biochemistry 25 (1986) 6917.
[60] M. Wahlgren, S. Welin-Klintström, T. Arnebrant, A. Askendal, H. Elwing, Colloids Surf. B 4 (1995) 23.
[61] V.B. Fainerman, S.A. Zholob, M. Leser, M. Michel, R. Miller, J. Colloid Interface Sci. 274 (2004) 496.
[62] G.M. Kamande, K.J. Cheng, J.A. Shelford, J. Baah, T.A. McAllister, J. Dairy Sci. 83 (2000) 536.
[63] S. Kerstens, B.S. Murray, E. Dickinson, Food Hydrocolloids 19 (2005) 625.
[64] H.C. Mahler, R. Müller, A. Delille, S. Matheus, W. Frieß, H.C. Mahler, Eur. J. Pharmaceut. Biopharmaceut. 59 (2005) 407.
[65] J.R. Potts, I.D. Campbell, Curr. Opin. Cell Biol. 6 (1994) 648.

[66] A.L. Main, T.S. Harvey, M. Baron, J. Boyd, I.D. Campbell, Cell 71 (1992) 671.
[67] A.R. Pickford, S.P. Smith, D. Staunton, J. Boyd, I.D. Campbell, EMBO J. 20 (2001) 1519.
[68] M.J. Williams, I. Phan, M. Baron, P.C. Driscoll, I.D. Campbell, Biochemistry 32 (1993) 7388.
[69] K. Gast, A.J. Modler, H. Damaschun, R. Kröber, G. Lutsch, D. Zirwer, G. Damaschun, R. Golbik, Eur. Biophys. J. 32 (2003) 710.
[70] N.M. Kad, S.L. Myers, D.P. Smith, D.A. Smith, S.E. Radford, N.H. Thomson, J. Mol. Biol. 330 (2003) 785.
[71] R. Khurana, J.R. Gillespie, A. Talapatra, L.J. Minert, C. Ionescu-Zanetti, I. Millett, A.L. Fink, Biochemistry 40 (2001) 3525.